AMERICAN SOCIETY FOR MICROBIOLOGY | mBio®

RESEARCH ARTICLE

Multiple Mechanisms for Copper Uptake by *Methylosinus trichosporium* OB3b in the Presence of Heterologous Methanobactin

Peng Peng,[a] Wenyu Gu,[a*] Alan A. DiSpirito,[b] Jeremy D. Semrau[a]

[a]Department of Civil and Environmental Engineering, University of Michigan, Ann Arbor, Michigan, USA
[b]Roy J. Carver Department of Biochemistry, Biophysics and Molecular Biology, Iowa State University, Ames, Iowa, USA

ABSTRACT Methanotrophs require copper for their activity as it plays a critical role in the oxidation of methane to methanol. To sequester copper, some methanotrophs secrete a copper-binding compound termed methanobactin (MB). MB, after binding copper, is reinternalized via a specific outer membrane TonB-dependent transporter (TBDT). *Methylosinus trichosporium* OB3b has two such TBDTs (MbnT1 and MbnT2) that enable *M. trichosporium* OB3b to take up not only its own MB (MB-OB3b) but also heterologous MB produced from other methanotrophs, e.g., MB of *Methylocystis* sp. strain SB2 (MB-SB2). Here, we show that uptake of copper in the presence of heterologous MB-SB2 can either be achieved by initiating transcription of *mbnT2* or by using its own MB-OB3b to extract copper from MB-SB2. Transcription of *mbnT2* is mediated by the N-terminal signaling domain of MbnT2 together with an extracytoplasmic function sigma factor and an anti-sigma factor encoded by *mbnI2* and *mbnR2*, respectively. Deletion of *mbnI2R2* or excision of the N-terminal region of MbnT2 abolished induction of *mbnT2*. However, copper uptake from MB-SB2 was still observed in *M. trichosporium* OB3b mutants that were defective in MbnT2 induction/function, suggesting another mechanism for uptake copper-loaded MB-SB2. Additional deletion of MB-OB3b synthesis genes in the *M. trichosporium* OB3b mutants defective in MbnT2 induction/function disrupted their ability to take up copper in the presence of MB-SB2, indicating a role of MB-OB3b in copper extraction from MB-SB2.

IMPORTANCE Methanotrophs play a critical role in the global carbon cycle, as well as in future strategies for mitigating climate change through their consumption of methane, a trace atmospheric gas much more potent than carbon dioxide in global warming potential. Copper uptake is critical for methanotrophic activity, and here, we show different approaches for copper uptake. This study expands our knowledge and understanding of how methanotrophs collect and compete for copper, and such information may be useful in future manipulation of methanotrophs for a variety of environmental and industrial applications.

KEYWORDS TonB-dependent transporter, copper, methanobactin, methanotroph

Methanotrophs, microbes that use methane as their sole carbon and energy source (1–3), have received increased attention as they play a critical role in controlling emissions of methane, a potent greenhouse gas with a global warming potential 28 times higher than carbon dioxide over a 100-year time frame (4). Interestingly, methanotrophic activity is strongly controlled by copper. More specifically, copper availability controls the expression and activity of alternative forms of the methane monooxygenase (MMO) that carries out the first step in methane oxidation (i.e., the conversion of methane to methanol) (5–9). There are two forms of MMO: the cytoplasmic or soluble methane monooxygenase (sMMO) and the membrane-bound or particulate methane monooxygenase (pMMO). Most methanotrophs can only express pMMO (1, 2), and its activity is strongly dependent on copper (5–9). A small number of methanotrophs can also express sMMO in addition to pMMO (10), and in these methanotrophs, the expression and activity of the two forms of MMO are dependent on copper availability. That is, there is a "copper switch" in which sMMO expression/activity is only

Editor Michael David Leslie Johnson, University of Arizona

Copyright © 2022 Peng et al. This is an open-access article distributed under the terms of the Creative Commons Attribution 4.0 International license.

Address correspondence to Jeremy D. Semrau, jsemrau@umich.edu.

*Present address: Wenyu Gu, Department of Civil and Environmental Engineering, Stanford University, Stanford, California, USA.

The authors declare no conflict of interest.

This article is a direct contribution from Jeremy D. Semrau, a Fellow of the American Academy of Microbiology, who arranged for and secured reviews by Colin Murrell, University of East Anglia, and Yin Chen, University of Warwick.

Received 8 August 2022
Accepted 1 September 2022
Published 21 September 2022

observed in the absence of copper, while pMMO expression/activity increases with increasing copper (11–13). In addition to controlling MMO expression and activity, copper also controls the formation of intracytoplasmic membrane of methanotrophic cells, as well as expression of genes involved in copper uptake (14, 15).

Due to the essential role of copper in methanotrophic physiology, some methanotrophs secrete a copper-binding compound or chalkophore named methanobactin (MB) for copper uptake. MBs are small (<1,350 Da) ribosomally synthesized posttranslationally modified polypeptides (RiPPS) that have high affinity and specificity for copper ($\sim 10^{20}$ to 10^{30} M^{-1}) (2, 16–25). The copper ligands of MB consist of nitrogen-containing heterocyclic rings and neighboring thioamide groups with posttranslational modifications (2, 16–20).

Methylosinus trichosporium OB3b is a model methanotrophic type strain that was first isolated and described in 1970 (26). The genome of *M. trichosporium* OB3b encodes both pMMO (encoded by *pmo*CAB or *pmo* operon) and sMMO (encoded by *mmoXYBZDC* or *mmo* operon) (27), and their expression and activity is controlled by copper availability (12). *M. trichosporium* OB3b can produce MB to sequester copper from its habitat environment. The responsible gene cluster (*mbn*) for MB biosynthesis includes *mbnA*, encoding the MB polypeptide precursor (*mbnA*), as well as several genes either with experimentally determined roles (e.g., *mbnBC* and *N*, involved in formation of heterocyclic rings) or imputed from bioinformatic analyses (e.g., *mbnM*, believed to be responsible for MB secretion), as well as some genes with as-yet-unknown roles (e.g., *mbnPH*, encoding a diheme cytochrome *c* oxidase and its partner protein) (19, 28–30).

Structural and bioinformatic analyses indicate that MB can be divided into two general groups: group I and II. Group I MBs are typically represented by MB from *M. trichosporium* OB3b (MB-OB3b). The primary structure of MB-OB3b includes two oxazolone rings with a disulfide bridge between two cysteine residues (Fig. S1A). Copper is chelated by the N- and S-ligands of the oxazolones and thioamides, respectively, forming a pyramid-like shape (17, 18, 31). Group II MBs are represented by the MB from *Methylocystis* sp. strain SB2 (MB-SB2). Unlike MB-OB3b, MB-SB2 has one oxazolone ring and one imidazolone ring (Fig. S1B). A disulfide bridge is absent from MB-SB2. MB-SB2 forms a hairpin shape upon binding copper via the N-ligand of the oxazolone/imidazolone and the S-ligand of thioamides (17, 21). Interestingly, recent phylogenetic analyses suggest that these two general groups can be further subdivided into at least five subgroups: groups IA, IB, IIA, IIB, and IIC (28). To date, 22 *mbn* gene clusters have been identified in methanotrophs belonging to the genera *Methylosinus* and *Methylocystis*; 10 of these encode group I MB (group IA: 6, group IB: 4), and 12 encode group II MB (group IIA: 6, group IIB: 5, group IIC: 1) (28).

It should be stressed that MBs are part of an extracellular mechanism for copper collection; i.e., after biosynthesis, MB must be secreted and subsequently reinternalized after binding copper. The mechanism of MB excretion is believed (but not conclusively shown) to occur via a multidrug export pump encoded by *mbnM*. MB uptake has been much more extensively characterized, with a TonB-dependent transporter (TBDT, encoded by *mbnT*) shown to be critical for reinternalization (32–34). In general, TBDTs consist of two conserved domains: one a barrel domain that forms the basic/main structure and the other a plug domain that is folded into the barrel interior (35). The plug domain functions to bind and transport specific compounds, such as MB, siderophores, vitamins, nickel complexes, and carbohydrates (35, 36). Some TBDTs also include a signaling domain at the N terminus that is involved in signal transmission to regulators (i.e., extracytoplasmic function [ECF] sigma and anti-sigma factors) for inducing specific gene(s) expression (e.g., TBDT genes) (36–39). Such TBDT signaling domain and (anti)-sigma factor-mediated regulation of gene(s) expression has been extensively studied in microbial ferric-siderophore uptake systems. It has been shown that upon binding of a specific siderophore to its TBDT transporter, a conformational change of the TBDT occurs that generates a signal that is transmitted to the anti-sigma factor via the signaling domain of the TBDT, leading to release of the ECF sigma factor into the cytoplasm. The released ECF sigma factor then enables binding of RNA polymerase to the promoter of specific gene(s), thereby initiating transcription (35, 37, 40).

Previously, it has been demonstrated that *M. trichosporium* OB3b has two MB uptake systems mediated by MbnT1 and MbnT2 responsible for uptake of homologous and heterologous

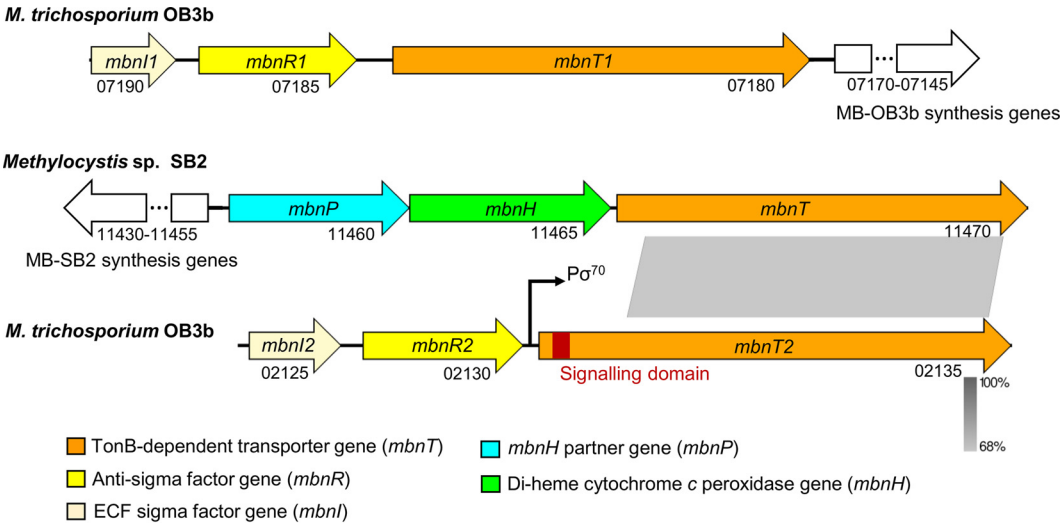

FIG 1 Comparison of the *mbnT* gene clusters of *M. trichosporium* OB3b and *Methylocystis* sp. SB2. Gene locus tags according to the genomes of *M. trichosporium* OB3b and *Methylocystis* sp. SB2 in NCBI under accession numbers NZ_CP023737 and NZ_CP091318, respectively, are indicated. The signaling domain encoding region of *mbnT2* (*M. trichosporium* OB3b) and the sequence identity of *mbnT2* and *mbnT* (*Methylocystis* sp. SB2) are indicated. The σ^{70} promoter (Pσ^{70}) region is indicated in the *mbnT2* gene clusters. The σ^{70} promoter was predicted using BPROM. The linear comparison figure was created using Easyfig (58). ECF, extracytoplasmic function.

MBs (MB-OB3b and MB-SB2), respectively (32–34). In this study, we demonstrate that *M. trichosporium* OB3b can take up copper from heterologous MB-SB2 via two different approaches. One is initiating transcription of MbnT2, which is collaboratively mediated by the N-terminal signaling domain of MbnT2 together with an ECF sigma and an anti-sigma factor (MbnI2 and MbnR2). The other approach is using its own MB-OB3b to extract copper from MB-SB2.

RESULTS

Comparison of the *mbnT2* and *mbnT* gene clusters in *M. trichosporium* OB3b and *Methylocystis* sp. SB2, respectively. To visualize the similarities and differences between the MB-SB2 uptake systems in *M. trichosporium* OB3b and *Methylocystis* sp. SB2, we first compared the corresponding *mbnT* gene clusters. The nucleic acid sequences of *mbnT2* and *mbnT* of *Methylocystis* sp. SB2 (*mbnT*-SB2) are 68% identical (Fig. 1). The main difference between *mbnT2* and *mbnT*-SB2 was found in the initial 5′ region. That is, *mbnT2* has an extension that is missing in *mbnT*-SB2 (Fig. 1). We speculated this extension region encodes a signaling domain involved in regulating expression of *mbnT2*. Indeed, two genes encoding an ECF sigma factor (*mbnI2*) and a putative membrane sensor (anti-sigma factor, *mbnR2*) that are commonly associated with TBDTs are immediately upstream of *mbnT2* (Fig. 1). In comparison, no such regulatory genes are colocated with *mbnT*-SB2 in the genome of *Methylocystis* sp. SB2. Rather, upstream of *mbnT*-SB2 are *mbnPH*. As noted above, these genes encode a diheme cytochrome *c* peroxidase and its partner protein and are not believed to have any regulatory function but are speculated to assist in MB maturation and/or facilitate copper release from MB (41) (Fig. 1).

The protein sequences of MbnT2 and MbnT-SB2 both contain leading signal peptides that are responsible for translocating the proteins to the outer cellular membrane (Fig. S2). Mature protein sequence of MbnT2 and MbnT-SB2 is obtained by removing the leading signal peptides from the original protein sequences (Fig. S3), with the overall amino acid identity of mature MbnT2 and MbnT-SB2 being 57%. Sequence alignment further indicated the presence and absence of the N-terminal signaling domain in MbnT2 and MbnT-SB2, respectively (Fig. 2; Fig. S3). The amino acid identity of the conserved domains—i.e., the "plug" (responsible for binding and transport of MB) and the "barrel" (responsible for forming the basic/main structure of MbnT2)—of MbnT2 and MbnT-SB2 were 69 and 61%, respectively.

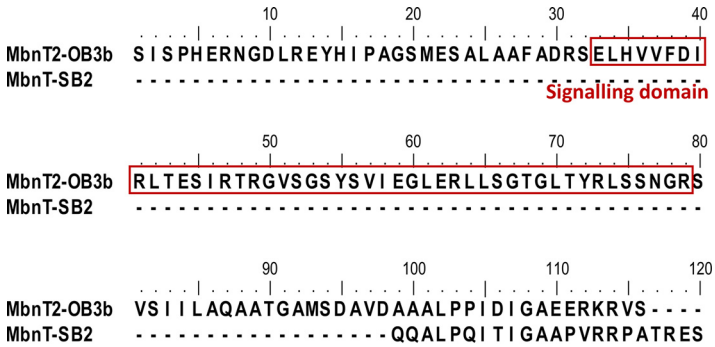

FIG 2 N-terminal extension (signaling domain) of mature MbnT2 protein of *M. trichosporium* OB3b compared to mature MbnT protein of *Methylocystis* sp. SB2. The signaling domain of MbnT2 was searched and predicted using Pfam database (59). The whole sequence alignment of different functional domains of MbnT2-OB3b and MbnT-SB2 are provided in the supplemental materials.

Copper uptake, MbnT2 and MMOs expression in *M. trichosporium* Δ*mbnI2R2* and Δ*mbnT2*-signal domain mutants. To explore the function and interaction of MbnI2R2 and the signaling domain of MbnT2, we constructed two mutants in *M. trichosporium* OB3b in which either *mbnI2R2* or the signaling domain encoding region of *mbnT2* was deleted (Fig. S4). The absence of *mbnI2R2* and the *mbnT2*-signaling domain in the constructed mutants was confirmed by PCR (Fig. S5) and sequencing (data not shown).

Copper associated with biomass was 7- to 8.5-fold higher in *M. trichosporium* OB3b wild type, Δ*mbnI2R2* and Δ*mbnT2*-signal domain mutants grown with copper (1 μM) versus without copper ($P < 0.01$; Fig. 3a to c). In the presence of 1 μM copper + 5 μM MB-SB2, copper associated with biomass in these two mutants was ~20% lower than when grown in the presence of copper (1 μM) alone (Fig. 3b and c). Such a difference in copper uptake by the mutants in the presence of copper (1 μM) alone versus copper (1 μM) + MB-SB2 (5 μM) was significant ($P < 0.05$) and was not observed in wild-type *M. trichosporium* OB3b (Fig. 3a).

mbnT2 was significantly downregulated in the presence versus the absence of copper (~3-fold; $P < 0.05$) in *M. trichosporium* wild type. *mbnT2*, however, was upregulated (90- to 290-fold; $P < 0.01$) in *M. trichosporium* OB3b wild type when grown in the presence of copper (1 μM) and MB-SB2 (5 μM) compared to the absence or presence of copper (34) (Fig. 3d). Similar to that found for wild-type *M. trichosporium* OB3b, the presence of copper reduced *mbnT2* expression in both *M. trichosporium* Δ*mbnI2R2* and Δ*mbnT2*-signal domain mutants (7 and 5-fold, $P < 0.01$). Unlike wild-type *M. trichosporium* OB3b, however, there was no significant difference in *mbnT2* expression in both *M. trichosporium* Δ*mbnI2R2* and Δ*mbnT2*-signal domain mutants grown with copper (1 μM) alone versus copper (1 μM) + MB-SB2 (5 μM) (Fig. 3d to f). Moreover, there was no significant difference in *mbnT* expression in *Methylocystis* sp. SB2 grown in the presence of copper (1 μM) alone versus copper (1 μM) + MB-SB2 (5 μM) (Fig. S6).

mmoX (encoding the 60-kDa α subunit of the sMMO hydroxylase) expression was over 3 orders of magnitude greater in *M. trichosporium* OB3b wild type, *M. trichosporium* OB3b Δ*mbnI2R2*, and Δ*mbnT2*-signal domain mutants grown in the absence of copper versus in the presence of copper (1 μM) ($P < 0.01$) (Fig. 3g to i). In the presence of copper + MB-SB2, *mmoX* expression in *M. trichosporium* OB3b wild type and Δ*mbnI2R2* and Δ*mbnT2*-signal domain mutants increased 1- to 2-fold compared to that found in the presence of 1 μM copper alone. Inversely, *pmoA* (encoding the 27-kDa β subunit of pMMO) expression in *M. trichosporium* OB3b wild type and Δ*mbnI2R2* and Δ*mbnT2*-signal domain mutants was ~6-fold lower in the absence versus in the presence of copper ($P < 0.05$). In the presence of copper (1 μM) + MB-SB2 (5 μM), *pmoA* expression in these mutants increased 1.5- to 2.5-fold over that observed in the presence of copper alone ($P < 0.05$; Fig. 3k and l). Such upregulation of *pmoA* in the presence of copper + MB-SB2 versus copper alone was not observed in the wild-type *M. trichosporium* OB3b (Fig. 3j).

These results showed that in the presence of copper and MB-SB2, *mbnT2* expression was induced in wild-type *M. trichosporium* OB3b. Such *mbnT2* induction was not observed

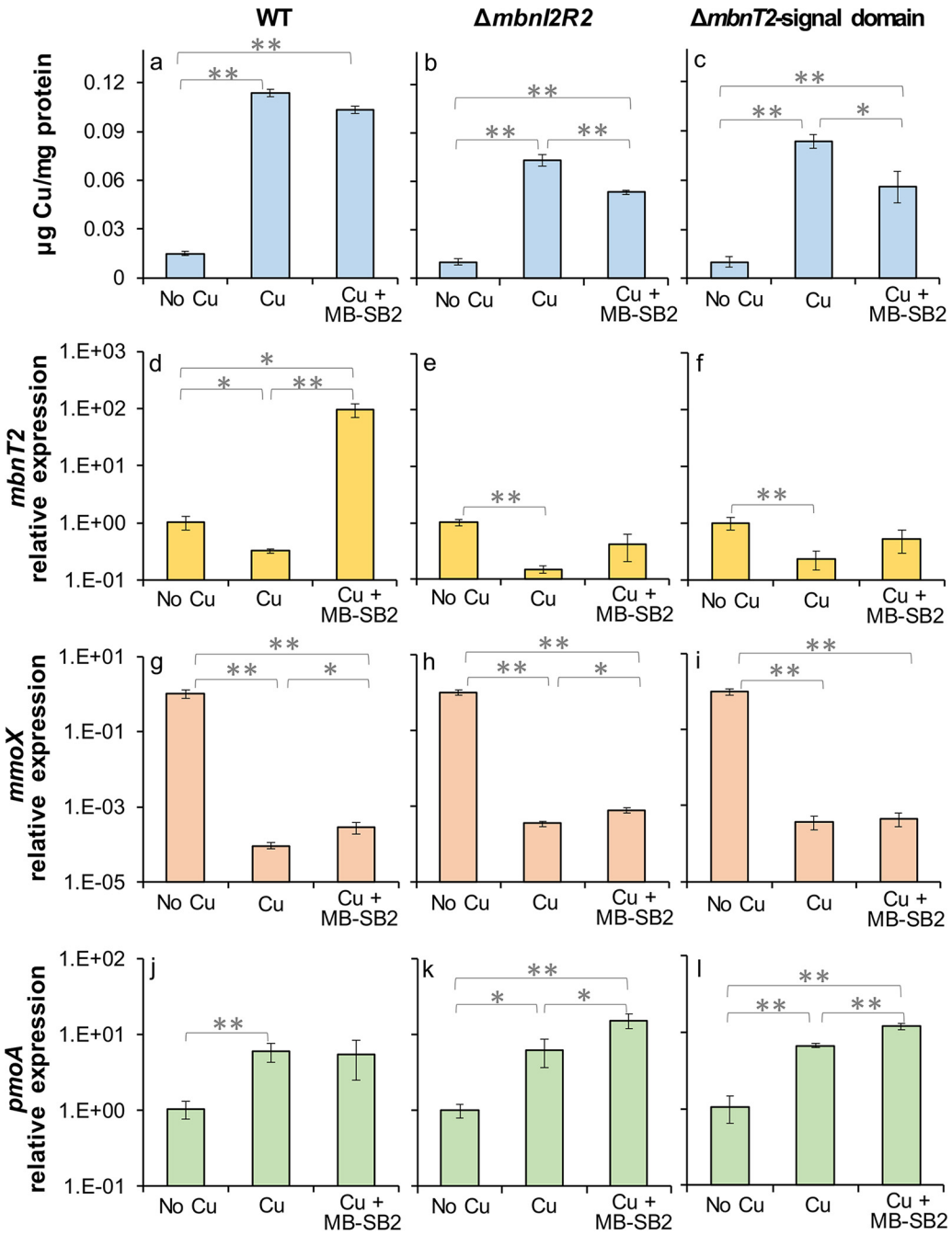

FIG 3 Copper associated with biomass and reverse transcription-quantitative PCR (RT-qPCR) analysis of the relative expression of *mbnT2*, *mmoX*, and *pmoA* in *M. trichosporium* OB3b wild type (WT) (a, d, g, and j) and Δ*mbnI2R2* (b, e, h, and k) and Δ*mbnT2*-signal domain (c, f, i, and l) mutants growing with no added Cu, 1 μM Cu, or 1 μM Cu + 5 μM MB-SB2. Error bars indicate standard deviations from triplicate biological cultures. *t* tests were performed for variance analysis between different growth conditions. *, $0.01 < P < 0.05$; **, $P < 0.01$.

in *M. trichosporium* OB3b Δ*mbnI2R2* and Δ*mbnT2*-signal domain mutants. However, the two mutants were still able to take up copper in the presence of MB-SB2.

***mbnT2* expression in *M. trichosporium mbnT1*::Gm^r.** *mbnT2* was also significantly upregulated (36-fold, $P < 0.01$) in a mutant of *M. trichosporium* OB3b in which the gene encoding the TBDT (MbnT1) responsible for MB-OB3b uptake was knocked out (*mbnT1*::Gm^r) (33) when grown in the presence of MB-OB3b (5 μM) compared to the absence of MB-OB3b (Fig. 4). In contrast, no significant different in *mbnT2* expression was observed in wild-type *M. trichosporium* OB3b grown with and without an extra supplement of MB-OB3b (5 μM) (Fig. 4).

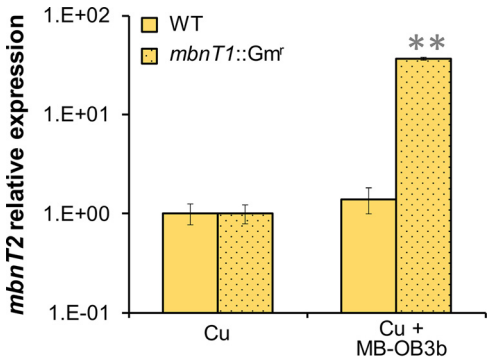

FIG 4 RT-qPCR analysis of the relative expression of *mbnT2* in *M. trichosporium* OB3b wild type (WT) and *mbnT1*::Gm^r mutant growing with 1 μM Cu or 1 μM Cu + 5 μM MB-OB3b. Error bars indicate standard deviations from triplicate biological cultures. *t* tests were performed for variance analysis between the growth conditions. **, $P < 0.01$.

Copper uptake and MMOs expression in *M. trichosporium* Δ*mbnAN*, Δ*mbnAN* Δ*mbnI2R2*, Δ*mbnAN* Δ*mbnT2*-signal domain, and Δ*mbnAN* Δ*mbnT2* mutants. To further explore the mechanism of copper uptake in the presence of MB-SB2 by the *M. trichosporium* Δ*mbnI2R2* and Δ*mbnT2*-signal domain mutants, we created three additional double mutants; i.e., we deleted *mbnI2R2*, the signaling domain region of *mbnT2*, and the entire *mbnT2* gene in a previously constructed mutant of *M. trichosporium* OB3b defective in production of its own MB-OB3b (i.e., the *M. trichosporium* Δ*mbnAN* mutant with its MB synthesis genes *mbnABCMN* deleted) (29) (Fig. S4). The deletion of both *mbnAN* and either *mbnI2R2*, *mbnT2*-signal domain, or *mbnT2* was confirmed by PCR (Fig. S5) and sequencing (data not shown).

Copper associated with biomass was 5- to 8-fold higher in *M. trichosporium* Δ*mbnAN*, Δ*mbnAN* Δ*mbnI2R2*, Δ*mbnAN* Δ*mbnT2*-signal domain, and Δ*mbnAN* Δ*mbnT2* mutants grown with copper versus without copper ($P < 0.01$; Fig. 5a to d). In the presence of copper + MB-SB2, copper associated with biomass in Δ*mbnAN* mutant was comparable to that in the presence of 1 μM copper alone (Fig. 5a), while in the double mutants (Δ*mbnAN* Δ*mbnI2R2*, Δ*mbnAN* Δ*mbnT2*-signal domain, and Δ*mbnAN* Δ*mbnT2*), copper associated with biomass decreased to that observed in the absence of copper (Fig. 5a to d).

Similar to wild-type *M. trichosporium* OB3b, *mbnT2* was significantly upregulated (75- to 240-fold; $P < 0.01$) in *M. trichosporium* Δ*mbnAN* mutant when grown in the presence of copper + MB-SB2 compared to the absence or presence of 1 μM copper alone (Fig. 5e). Such upregulation was not observed in *M. trichosporium* OB3b Δ*mbnAN* Δ*mbnI2R2* mutant, in which *mbnT2* expression was invariant when grown with or without copper and/or MB-SB2 (Fig. 5f). *mbnT2* expression was uniformly low in the Δ*mbnAN* Δ*mbnT2*-signal domain mutant under all conditions but was significantly (2- to 3-fold) less when this mutant was grown in the presence of copper versus either the absence of copper or copper added in the presence of + MB-SB2 (5 μM) (Fig. 5g).

mmoX expression was 3 to 4 orders of magnitude higher in *M. trichosporium* Δ*mbnAN*, Δ*mbnAN* Δ*mbnI2R2*, Δ*mbnAN* Δ*mbnT2*-signal domain, and Δ*mbnAN* Δ*mbnT2* mutants grown in the absence of copper versus presence of 1 μM copper ($P < 0.01$). In the presence of copper + MB-SB2, *mmoX* expression in Δ*mbnAN* decreased to the same level of that in the presence of copper, while for the other double mutants, the *mmoX* expression level was equivalent to that observed in the absence of copper (Fig. 5h to k).

pmoA expression in the *M. trichosporium* Δ*mbnAN*, Δ*mbnAN* Δ*mbnI2R2*, Δ*mbnAN* Δ*mbnT2*-signal domain, and Δ*mbnAN* Δ*mbnT2* mutants decreased 2- to 3-fold in the absence versus in the presence of copper. In the presence of copper + MB-SB2, *pmoA* expression in Δ*mbnAN* was comparable to that with copper (1 μM) alone. *pmoA* expression slightly decreased (1.2- to 2.5-fold) in all double mutants when grown with copper + MB-SB2 versus copper alone (Fig. 5l to o), although such differences were not significant ($P > 0.05$). Collectively, these results indicated that copper bound to MB-SB2 was unavailable to *M. trichosporium* mutants defective in both MB-OB3b production and MbnT2

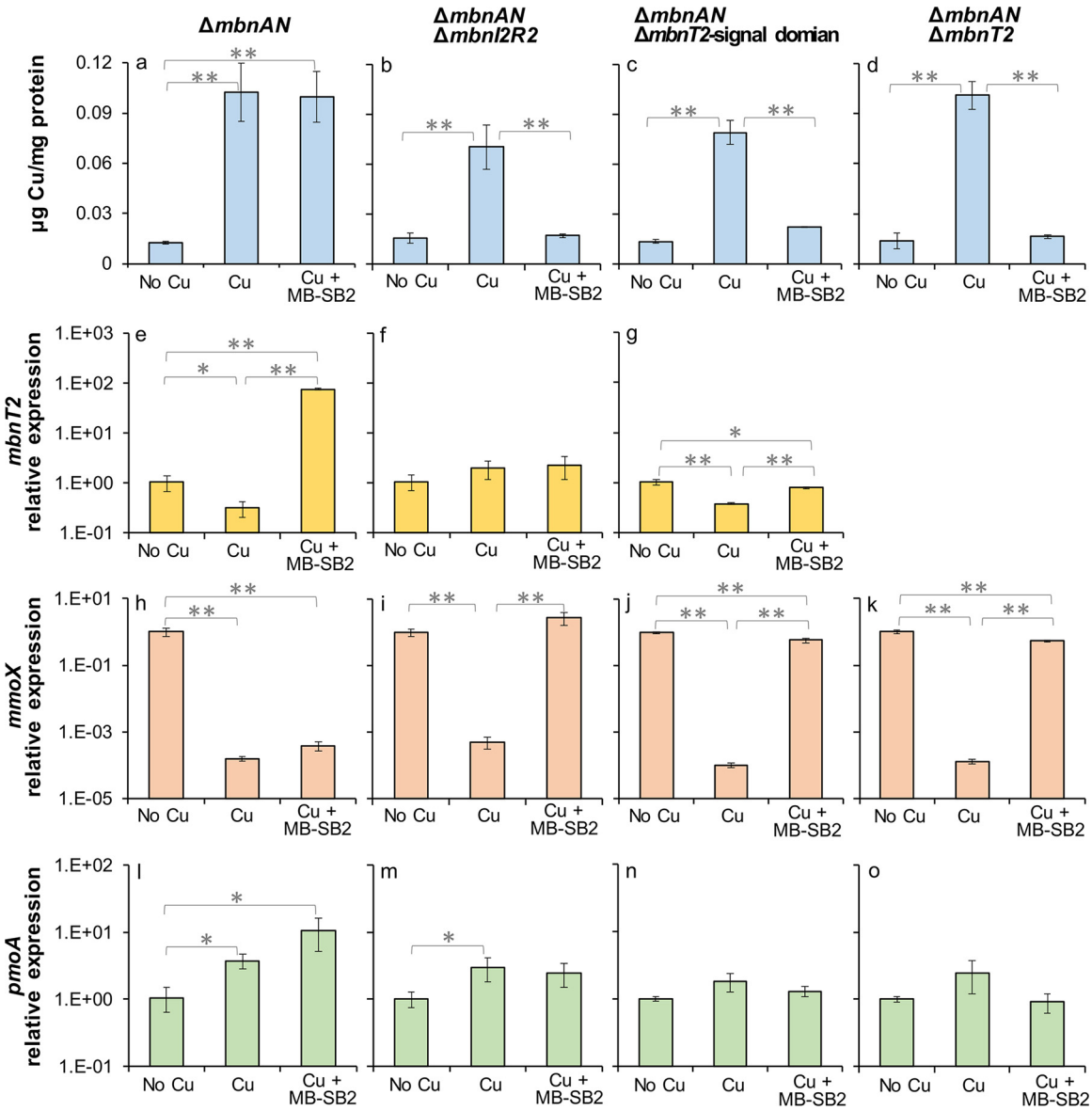

FIG 5 Copper associated with biomass and RT-qPCR analysis of the relative expression of *mbnT2*, *mmoX*, and *pmoA* in *M. trichosporium* OB3b Δ*mbnAN* (a, e, h, and l), Δ*mbnAN* Δ*mbnI2R2* (b, f, i, and m), Δ*mbnAN* Δ*mbnT2*-signal domain (c, g, j and n), or Δ*mbnAN* Δ*mbnT2* (d, k, and o) mutants growing with no added Cu, with 1 μM Cu, or with 1 μM Cu + 5 μM MB-SB2. Error bars indicate standard deviations from triplicate biological cultures. *t* tests were performed for variance analysis between different growth conditions. *, $0.01 < P < 0.05$; **, $P < 0.01$.

induction/function. Moreover, native MB production was essential for copper uptake in *M. trichosporium* mutants in which either *mbnT2/mbnI2R2* has been deleted or the internal signaling domain has been removed.

Copper transfer/extraction between MB-OB3b and MB-SB2. To investigate how MB-OB3b can facilitate copper uptake by the *M. trichosporium* mutants that cannot properly regulate *mbnT2* expression (i.e., Δ*mbnI2R2* and Δ*mbnT2*-signal domain mutants), we characterized the ability of the *M. trichosporium* Δ*mbnAN* Δ*mbnT2* to collect copper in the presence of exogenous MB-OB3b. When Δ*mbnAN* Δ*mbnT2* was grown in the presence of copper-loaded MB-SB2 (Cu-MB-SB2) and MB-OB3b (see Materials and Methods for a detailed description of experimental protocols), copper associated with biomass was ~5-fold higher ($P < 0.01$) than in the absence of added MB-OB3b (Fig. 6a). In addition, *mmoX* expression was over 3 orders of magnitude lower ($P < 0.01$) in the presence of MB-OB3b, while *pmoA* expression was 2.5-fold higher ($P < 0.05$) (Fig. 6c and e). Moreover, copper associated with biomass in Δ*mbnAN* Δ*mbnT2* was only slightly (~20%) ($P < 0.05$)

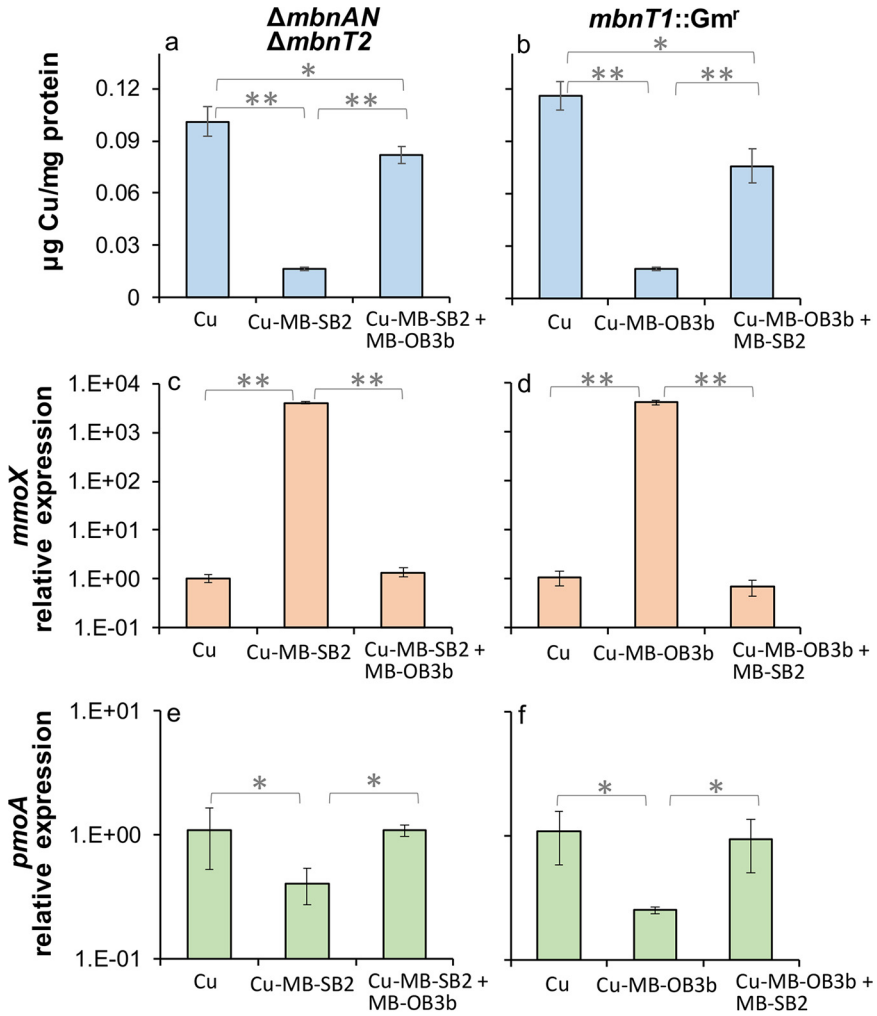

FIG 6 Copper associated with biomass and RT-qPCR analysis of the relative expression of *mmoX* and *pmoA* in *M. trichosporium* Δ*mbnAN* Δ*mbnT2* (a, c, and e) and *mbnT1*::Gm^r (b, d, and f) mutants growing with 1 μM Cu, 1 μM Cu-MB-SB2/OB3b or 1 μM Cu-MB-SB2/OB3b + 5 μM MB-OB3b/SB2. Error bars indicate standard deviations from triplicate biological cultures. *t* tests were performed for variance analysis between different growth conditions. *, $0.01 < P < 0.05$; **, $P < 0.01$.

lower when grown with Cu-MB-SB2 + MB-OB3b (5 μM) versus copper alone (Fig. 6a). *mmoX* and *pmoA* expression were comparable when growing this mutant with Cu-MB-SB2 + MB-OB3b versus copper alone (Fig. 6c and e). These results suggest that MB-OB3b can extract copper from Cu-MB-SB2. We further investigated this to determine whether MB-SB2 can extract copper from Cu-MB-OB3b in *M. trichosporium* OB3b *mbnT1*::Gm^r that cannot take up copper when bound to MB-OB3b (Cu-MB-OB3b) (33). When *mbnT1*::Gm^r was growing in the presence of Cu-MB-OB3b + MB-SB2, copper associated with biomass was 4.7-fold higher ($P < 0.01$), *mmoX* expression was over 3 orders of magnitude lower ($P < 0.01$), and *pmoA* expression was 3.8-fold higher ($P < 0.05$) versus growing with Cu-MB-OB3b alone (Fig. 6b, d, and f). Moreover, copper associated with biomass in *mbnT1*::Gm^r was ~30% less ($P < 0.05$) when grown with Cu-MB-OB3b + MB-SB2 versus copper alone (Fig. 6a). *mmoX* and *pmoA* expression was comparable when growing this mutant with Cu-MB-OB3b + MB-SB2 versus copper alone (Fig. 6d and f). These results further indicate that MB-SB2 can extract copper from Cu-MB-OB3b; i.e., it appears that MB-OB3b and MB-SB2 can extract copper from the Cu-MB complex of their counterpart.

Previous studies have shown the copper affinity for both MB-OB3b and MB-SB2 varies depending on copper to MB molar ratio (16, 42). To illustrate copper binding by either form of MB, UV-visible spectrophotometry provides a simple and convenient assay as the magnitude

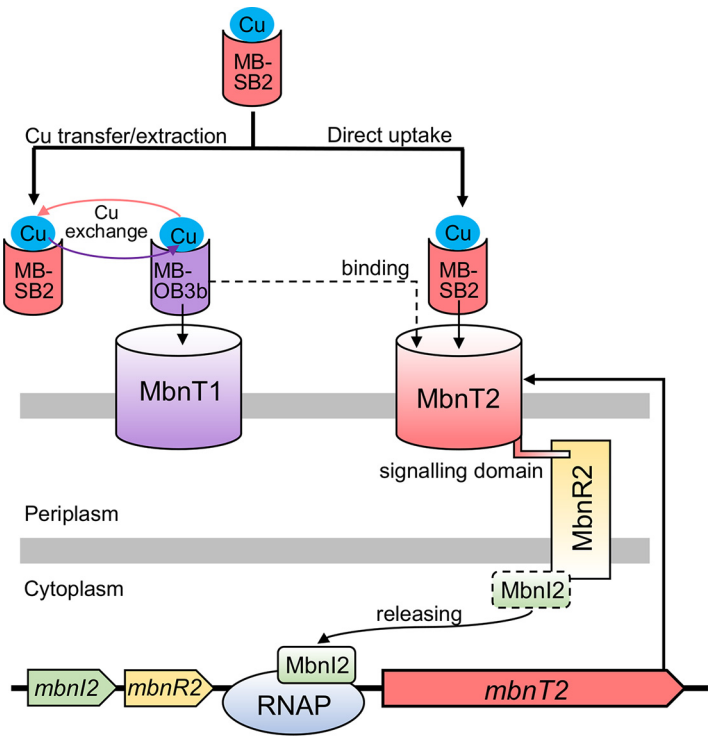

FIG 7 Proposed mechanisms for copper uptake from Cu-MB-SB2 by *M. trichosporium* OB3b via either copper exchange between MB-OB3b and MB-SB2 or initiating transcription of MbnT2 that is mediated by the signaling domain of MbnT2 and ECF sigma factor (MbnI2) and anti-sigma factor (MbnR2). MbnI2 is released from MbnR2 to recruit RNA polymerase (RNAP) upon binding of MB-SB2 or MB-OB3b to MbnT2 that generates a signal transmitted to MbnR2.

and wavelength of absorption maxima of the heterocyclic rings decreases with increasing copper (Fig. S7A and B). That is, a 10-nm blue shift is observed in the absorption maxima of the C-terminal oxazolone ring of both MB-OB3b and MB-SB2 (344 to 334 nm and 336 to 326 nm, respectively) (Fig. S7A and B) as copper is added. These assays can be extended to monitor copper exchange between MB-OB3b and MB-SB2. The addition of metal free MB-OB3b to an 80% saturated solution of MB-SB2 resulted in an incremental red shift in the oxazolone group of MB-SB2, demonstrating copper loss by MB-SB2 and copper uptake by MB-OB3b (Fig. S7C). Conversely, the incremental addition of metal free MB-SB2 to an 80% copper saturated solution of MB-OB3b resulted in an incremental blue shift in the oxazolone group of MB-SB2, demonstrating copper uptake by MB-SB2 from copper containing MB-OB3b (Fig. S7D).

DISCUSSION

In an earlier study (34), we identified a second MB uptake system (mediated by MbnT2) in *M. trichosporium* OB3b that is responsible for uptake of heterologous MB produced from *Methylocystis* sp. SB2 and determined that the expression of *mbnT2* is induced by MB-SB2. Here, we show that such upregulation is dependent on a signaling domain at the N terminus of MbnT2. It appears that this domain acts in concert with an ECF sigma factor and an anti-sigma regulator (MbnI2 and MbnR2, respectively) that are encoded by genes immediately upstream of *mbnT2*. Such a signaling domain is absent in MbnT of *Methylocystis* sp. SB2, as well as these sigma and anti-sigma factor-encoding genes not associated with *mbnT* in *Methylocystis* sp. SB2 (28). This suggests that MbnT expression in *Methylocystis* sp. SB2 is not regulated by MB-SB2, as was found in *M. trichosporium* OB3b. Indeed, MbnT expression in *Methylocystis* sp. SB2 is not upregulated by the exogenous addition of MB-SB2 (Fig. S6).

TBDT and ECF sigma factor and anti-sigma regulator-mediated gene regulation has been extensively studied in microbial ferric-siderophore uptake systems (36, 37). Accordingly, the induction of gene expression by MB-SB2 in *M. trichosporium* OB3b can be proposed as follows (Fig. 7): (i) the binding of MB-SB2 to MbnT2 causes a conformational change of the

barrel and plug domains of MbnT2; (ii) the signaling domain of MbnT2 then transduces the signal by interacting with the C-terminal domain of the inner membrane anti-sigma factor MbnR2; (iii) MbnR2 subsequently releases the ECF sigma factor MbnI2 into the cytoplasm to recruit the core RNA polymerase (RNAP); and finally, (iv) MbnI2 promotes binding of the RNAP to the promoter of *mbnT2*, thereby initiating transcription.

It has been demonstrated that ferric-siderophore binding to the corresponding TBDT alone is sufficient for signal generation and transcriptional induction. That is, transport of the ferric-siderophore is not necessary for the signal transmission process (39, 43, 44). Interestingly, we found *mbnT2* can also be induced in *M. trichosporium mbnT1*::Gm^r in the presence of MB-OB3b (Fig. 4) (*mbnT1*::Gm^r is unable to take up MB-OB3b due to the disruption of MbnT1). Such MB-OB3b-initialized *mbnT2* induction is likely due to the nonspecific binding of MB-OB3b to MbnT2. It has been previously found that MB-OB3b can not only bind to MbnT1 that is responsible for MB-OB3b uptake (32, 33) but also can bind to MbnT of *Methylocystis rosea* SV97 (MbnT-SV97) (32). MbnT2 shares high identity (57%) and similarity (E value: 0) with MbnT-SV97 (moreover, the overall identity of MbnT-SV97 and MbnT-SB2 is 93%) (data not shown). Due to the high similarity between MbnT2, MbnT-SV97, and MbnT-SB2, it is likely that MB-OB3b can also bind to MbnT2 and thereby generate a signal to initialize the transcription of *mbnT2*. MB-OB3b initialized transcription of *mbnT2* is not observed in wild-type *M. trichosporium* OB3b, indicating specific binding (and uptake) of MB-OB3b to its cognate transporter MbnT1 rather than weaker nonspecific binding of MB-OB3b to MbnT2 in wild-type *M. trichosporium* OB3b. It should be noted that MbnT2 cannot take up/transport MB-OB3b as MbnT1 is the only TBDT for MB-OB3b uptake in *M. trichosporium* OB3b (33) (Fig. 6b).

An N-terminal signaling domain is also found in MbnT1 of *M. trichosporium* OB3b. Moreover, ECF sigma and anti-sigma factors encoding genes (*mbnI1* and *mbnR1*) are also adjacent to *mbnT1* (Fig. 1). Due to the similar structure of MbnT1 and MbnT2, as well as the genetic organization of the *mbnT1* and *mbnT2* gene clusters, it is reasonable to speculate that binding of MB-OB3b to MbnT1 should also generate a signal to release MbnI1 and thereby initialize transcription of MbnT1. However, unlike MbnT2, MbnT1 expression is not controlled by MB-OB3b (34). Rather, MbnT1 is constitutively expressed. That is, the expression of MbnT1 is invariant in *M. trichosporium* OB3b grown with and without exogenous MB-OB3b (34). MbnI1 might be responsible for regulating expression of other functional genes rather than *mbnT1*. Previous studies indicate that the regulon of TBDT-mediated ECF sigma factor is rather broad (40). For example, the siderophore uptake system of *Pseudomonas aeruginosa* PAO1 consists of a siderophore TBDT receptor (FpvA), an anti-sigma factor FpvR, and the two ECF sigma factors FpvI and PvdS. In this cascade, the binding of siderophore transmits a signal to release FpvI and PvdS, which control the expression of over 80 genes, including *fpvA* (the ferric-siderophore transporter encoding gene), ferric-siderophore biosynthesis genes, transporter genes for heme uptake, and small RNA genes (40, 42, 45). Hence, it is possible that MbnI1 is involved in regulating as-of-yet-unknown gene(s) in *M. trichosporium* OB3b. Moreover, in addition to regulating *mbnT2* expression, MbnI2 might also be involved in regulating other (yet-unknown) functional gene(s). Further research is clearly needed to address these questions.

Herein, we show that MbnI2, MbnR2, and MbnT2 signaling domain-mediated transcriptional induction of MbnT2 is essential for MB-SB2 uptake by *M. trichosporium* OB3b. As demonstrated previously (34) and together with this study, MbnT2 is the only TBDT responsible for MB-SB2 transport/uptake in *M. trichosporium* OB3b. However, copper bound to MB-SB2 (Cu-MB-SB2) is still available for *M. trichosporium* OB3b mutants that cannot properly regulate *mbnT2* expression (Fig. 3). The production of MB-OB3b apparently plays a key role in copper uptake from Cu-MB-SB2 by the mutants defective in *mbnT2* expression or function, as deletion of *mbnAN* genes in these mutants disrupted their ability to take up copper from Cu-MB-SB2 (Fig. 5). That is, in the *M. trichosporium* OB3b mutant that can neither take up MB-SB2 nor produce MB-

OB3b (i.e., the Δ*mbnAN* Δ*mbnT2* mutant), adding MB-OB3b enabled this mutant to extract copper from Cu-MB-SB2 (Fig. 6a, c, and e). Likewise, in a *M. trichosporium* OB3b mutant that cannot take up MB-OB3b (i.e., *mbnT1*::Gm^r mutant), adding MB-SB2 enables this mutant to extract copper from Cu-MB-OB3b (Fig. 6b, d and f). Intriguingly, the exchange of copper between different forms of MB can occur, but such an exchange is concentration dependent (Fig. S7C and D). Clearly, interactions between methanotrophs for copper and competition for copper binding by MBs are much more complicated than initially presumed, and much more work is warranted to investigate these phenomena.

In any regard, copper uptake using MBs is an important mechanism for methanotrophs to collect this essential trace element from the environment lack of bioavailable copper. For example, MB-OB3b can extract copper from copper-sulfide minerals typically assumed to be biologically unavailable (46). Here, we demonstrate that the model methanotroph *M. trichosporium* OB3b can not only secrete and uptake its own MB but also has developed multiple mechanisms to take up copper in the presence of heterologous methanobactin MB-SB2, including initiating transcription of an alternative TBDT. A survey of available methanotrophic genomes shows a similar cooccurrence of alternative TBDTs and regulatory systems for heterologous MB uptake among MB-producing methanotrophs, especially group I MB-producing methanotrophs (Table S1). Interestingly, signaling domains are also found in TBDTs potentially responsible for heterologous MBs uptake in methanotrophs that produce group I MB, and sigma and anti-sigma encoding genes are adjacent to the TBDT genes (Table S1). Such genetic features suggest a similar regulatory mechanism of these TBDTs compared to MbnT2 in *M. trichosporium* OB3b. Moreover, all currently identified group I MB-producing methanotrophs express alternative MMOs (i.e., pMMO and sMMO). Together with the MbnT (responsible for their own/homologous MB uptake) of these methanotrophs, these TBDTs may also be involved in regulating the expression of alternative MMOs (i.e., the canonical "copper switch") in these methanotrophs as previously demonstrated in *M. trichosporium* OB3b (i.e., MbnT1 and MbnT2 comedicated copper switch) (34). Further studies are needed to investigate the regulation and functions of these TBDTs in MB uptake and methane metabolism (i.e., copper switch).

MATERIALS AND METHODS

MB isolation. MBs from *M. trichosporium* OB3b and *Methylocystis* sp. strain SB2 were isolated from their spent media as previously described by Bandow et al. (47). The purity of the isolated methanobactins was determined by high-performance liquid chromatography (HPLC) as described previously (48).

Growth conditions. *M. trichosporium* OB3b and constructed mutants (Table 1) were grown in nitrate mineral salt (NMS) medium (26) with or without 1 μM $CuCl_2$. *Methylocystis* sp. SB2 was grown in NMS medium with 1 μM $CuCl_2$. Methane and air were added at a methane-to-air ratio of 1:2. The cultures were incubated in dark at 30°C. Liquid cultures were grown in 250-mL sidearm Erlenmeyer flasks with 20 to 30 mL NMS medium with shaking at 200 rpm. MB from *M. trichosporium* OB3b or *Methylocystis* sp. SB2 were filter sterilized and added to NMS medium at final concentration of 5 μM as described previously (49). Solid NMS medium was supplemented with 1.2% agar. Growth was monitored by measuring the optical density at 600 nm (OD_{600}) with a Genesys 20 visible spectrophotometer (Spectronic Unicam, Waltham, MA). Triplicate biological cultures were harvested at middle to late exponential phase for OD_{600} measurement, transcriptional analysis of specific gene expression, and metal distribution. *Escherichia coli* was grown in Luria-Bertani broth (LB) at 37°C with or without a supplement of 25 μg/mL kanamycin.

Construction of the *M. trichosporium* OB3b Δ*mbnI2R2*, Δ*mbnT2*-signal domain mutants. *mbnI2R2* and *mbnT2*-signal domain were deleted in *M. trichosporium* OB3b wild type using a previously described protocol (50) with modifications. Briefly, upstream and downstream regions of the respective gene (arms A and B, respectively) were PCR amplified using the arm primers listed in Table S2. Arms A and B were digested with the restriction enzymes and ligated together to form arm AB, which was subsequently inserted into the pK18mob*sacB* mobilizable suicide vector (Fig. S4) (51). The pK18mob*sacB* vector with arm AB was transferred to *E. coli* TOP10 (Invitrogen, Carlsbad, CA). Plasmid was extracted from transformed *E. coli* Top10 using a plasmid mini kit (Qiagen, Hilden, Germany) following the manufacturer's instructions. The extracted plasmid was then transferred to *E. coli* S17-1 (52). Conjugation of *E. coli* S17-1 carrying the constructed vector with *M. trichosporium* OB3b was performed as described by Martin and Murrell (53). Transconjugants were grown on NMS plates supplemented with 25 μg/mL kanamycin and 10 μg/mL nalidixic acid. One kanamycin-resistant transconjugant colony (generated after 10 days incubation) was transferred to an NMS plate with kanamycin (25 μg/mL), incubated for 7 days, and subsequently transferred to an NMS plate with 2.5% sucrose (mass/volume). Sucrose-resistant colonies were generated after 10 days of incubation and were screened for mutation with deletion of *mbnI2R2* and *mbnT2*-signal domain by colony PCR using the checking primers (Table S2). Successful deletion mutation was further confirmed by PCR with DNA extracted from the mutant using the DNeasy PowerSoil Pro kit (Qiagen, Hilden, Germany) following the manufacturer's instructions.

TABLE 1 Bacterial strains used in this study

Strain	Description/genotype	Reference
M. trichosporium OB3b	Wild type	26
Methylocystis sp. strain SB2	Wild type	60
M. trichosporium mbnT1::Gm^r	*mbnT1* marker exchanged mutant with gentamicin resistance gene	33
M. trichosporium Δ*mbnAN*	*mbnAN* deleted	29
M. trichosporium Δ*mbnT2*	*mbnT2* deleted	34
M. trichosporium Δ*mbnI2R2*	*mbnI2R2* deleted	This work
M. trichosporium Δ*mbnT2*-signal domain	*mbnT2* signal domain encoding region deleted	This work
M. trichosporium Δ*mbnAN* Δ*mbnI2R2*	*mbnAN* and *mbnI2R2* deleted	This work
M. trichosporium Δ*mbnAN* Δ*mbnT2*-signal domain	*mbnAN* and *mbnT2* signal domain encoding region deleted	This work
M. trichosporium Δ*mbnAN* Δ*mbnT2*	*mbnAN* and *mbnT2* deleted	This work
E. coli TOP10	Strain used for plasmid construction and cloning. F$^-$ *mcrA* Δ(*mrr-hsdRMS-mcrBC*) Φ80*lacZ*ΔM15 Δ*lacX*74 *recA1 araD139* Δ(*ara leu*) 7697 *galU galK rpsL* (Str^r)	Invitrogen
E. coli S17-1	Conjugative donor; *recA1 thi pro hsdR*-RP4-2Tc::Mu Km::Tn7	51

Construction of the *M. trichosporium* OB3b Δ*mbnAN* Δ*mbnI2R2*, Δ*mbnAN* Δ*mbnT2*-signal domain, and Δ*mbnAN* Δ*mbnT2* mutants. To construct *M. trichosporium* OB3b mutants with double deletion of MB synthesis genes and *mbnI2R2* or *mbnT2*-signal domain or *mbnT2*, the previously constructed *M. trichosporium* OB3b mutant with its MB biosynthesis genes *mbnABCMN* deleted (Δ*mbnAN* mutant) (29) was used as the conjugation acceptor. That is, *mbnI2R2*, *mbnT2*-signal domain, and *mbnT2* were deleted in *M. trichosporium* OB3b Δ*mbnAN* mutant. The pK18mob*sacB* vector with arms targeting the homologous regions of *mbnI2R2*, *mbnT2*-signal domain, and *mbnT2* were obtained from this study (described above) or from the previous study (34). Conjugation, growing of the transconjugates, and selection of the double deletion mutants were performed as outlined above.

Copper competition and transfer between MBs. Copper-bound MB complexes (Cu-MB-OB3b/SB2) were prepared by mixing 1 μM $CuCl_2$ and 5 μM MB-OB3b/SB2 in NMS medium followed by incubating in the dark at 30°C with shaking at 200 rpm for 1 h. *M. trichosporium* Δ*mbnAN* Δ*mbnT2* (this study) and *mbnT1*::Gm^r mutants (33) were used for the study of copper competition and transfer between MBs. Δ*mbnAN* Δ*mbnT2* and *mbnT1*::Gm^r were grown in NMS medium containing 1 μM Cu-MB-SB2 + 5 μM MB-OB3b (Δ*mbnAN* Δ*mbnT2* mutant) or Cu-MB-OB3b + 5 μM MB-SB2 (*mbnT1*::Gm^r mutant). Δ*mbnAN* Δ*mbnT2* and *mbnT1*::Gm^r were also grown in NMS medium containing 1 μM Cu alone as positive controls and grown in 1 μM Cu-MB-SB2 alone (Δ*mbnAN* Δ*mbnT2* mutant) or 1 μM Cu-MB-OB3b alone (*mbnT1*::Gm^r mutant) as negative controls. Cells of the mutants were collected at the middle to late exponential growth phase for RNA isolation and copper measurement.

Copper titration of MB-OB3b and MB-SB2 were determined as described by Choi et al. (16) and Bandow et al. (54), respectively. To obtain 80% copper saturated 50 nmol (50 μM) MB-OB3b or 50 nmol (50 μM) MB-SB2 were mixed with 40 nmol (40 μM) $CuCl_2$ and determined by the UV-visible absorption spectra. Copper extraction from 80% copper saturated MB-OB3b or MB-SB2 was determined by monitoring the UV-visible spectral changes in the oxazolone group of MB-SB2 following the addition of MB-SB2 or MB-OB3b.

RNA isolation and reverse transcription-quantitative PCR (RT-qPCR). RNA isolation was performed with a bead-beating procedure followed by column purification using an RNeasy mini kit (Qiagen, Hilden, Germany) as described before (55). Genomic DNA was removed from the column with RNase-free DNase (Qiagen, Hilden, Germany) treatment. The absence of genomic DNA was confirmed by 16S rRNA gene targeted PCR with extracted RNA samples as the templates. The purified RNA was quantified using a NanoDrop 1000 spectrophotometer (Thermo Scientific, Wilmington, DE). cDNA was synthesized from 200 ng total RNA using SuperScript III reverse transcriptase (Invitrogen, Carlsbad, CA) following the manufacturer's instructions.

RT-qPCR assays were performed to determine the relative expression of the *mbnT2*, *pmoA*, and *mmoX* in *M. trichosporium* OB3b and mutant strains grown in the presence or absence of copper and/or methanobactins. RT-qPCR was performed using the iTaq Universal SYBR green Supermix (Bio-Rad, Hercules, CA) with 96-well PCR plates on a CFX Connect real-time PCR detection system (Bio-Rad, Hercules, CA). The RT-qPCR program was: 95°C for 10 min, followed by 40 cycles of 95°C for 15 s, 56°C for 30 s, and 72°C for 30 s. Melting curves were measured from 65 to 95°C with increments of 0.5°C and 10 s at each step. Transcription of the targeted genes was determined using cDNA as the template. The transcript levels were calculated by relative quantification using the $2^{-\Delta\Delta CT}$ method (56) with the 16S rRNA gene as the reference gene (57).

Metal analysis. Cells of *M. trichosporium* OB3b and the mutant strains grown under different conditions were collected and acid digested as described previously (33, 57). Copper associated with biomass was subsequently analyzed using an inductively coupled plasma mass spectrometer (ICP-MS; Agilent Technologies, Santa Clara, CA).

Data availability. The materials and data generated in this study will be made available upon reasonable request to the corresponding author.

SUPPLEMENTAL MATERIAL

Supplemental material is available online only.

FIG S1, DOCX file, 0.3 MB.

FIG S2, DOCX file, 0.3 MB.

FIG S3, DOCX file, 0.1 MB.

FIG S4, DOCX file, 0.1 MB.
FIG S5, DOCX file, 0.3 MB.
FIG S6, DOCX file, 0.02 MB.
FIG S7, PDF file, 0.4 MB.
TABLE S1, DOCX file, 0.03 MB.
TABLE S2, DOCX file, 0.02 MB.

ACKNOWLEDGMENTS

This research was supported by U.S. Department of Energy Office of Science grant DE-SC0020174 (to J.D.S. and A.A.D.). The funders had no role in study design, data collection and interpretation, or the decision to submit the work for publication.

We thank Christina S. Kang-Yun for constructive discussion and suggestions on mutant construction.

We declare no conflict of interest.

REFERENCES

1. Kalyuzhnaya MG, Gomez OA, Murrell JC. 2019. The methane-oxidizing bacteria (methanotrophs), p 245–278. *In* McGenity TJ (ed), Taxonomy, genomics and ecophysiology of hydrocarbon-degrading microbes. Springer Nature, Cham, Switzerland.
2. Semrau JD, DiSpirito AA, Gu W, Yoon S. 2018. Metals and methanotrophy. Appl Environ Microbiol 84:e02289-17. https://doi.org/10.1128/AEM.02289-17.
3. Semrau JD, DiSpirito AA, Yoon S. 2010. Methanotrophs and copper. FEMS Microbiol Rev 34:496–531. https://doi.org/10.1111/j.1574-6976.2010.00212.x.
4. Intergovernmental Panel on Climate Change. 2013. Contribution of working group I to the fifth assessment report of the Intergovernmental Panel on Climate Change. *In* Climate change 2013: the physical science basis. Cambridge University Press, New York, NY.
5. Balasubramanian R, Smith SM, Rawat S, Yatsunyk LA, Stemmler TL, Rosenzweig AC. 2010. Oxidation of methane by a biological dicopper centre. Nature 465:115–119. https://doi.org/10.1038/nature08992.
6. Lieberman RL, Rosenzweig AC. 2005. Crystal structure of a membrane-bound metalloenzyme that catalyses the biological oxidation of methane. Nature 434:177–182. https://doi.org/10.1038/nature03311.
7. Martinho M, Choi DW, DiSpirito AA, Antholine WE, Semrau JD, Münck E. 2007. Mössbauer studies of the membrane-associated methane monooxygenase from *Methylococcus capsulatus* Bath: evidence for a diiron center. J Am Chem Soc 129:15783–15785. https://doi.org/10.1021/ja077682b.
8. Nguyen H, Shiemke AK, Jacobs SJ, Hales BJ, Lidstrom ME, Chan SI. 1994. The nature of the copper ions in the membranes containing the particulate methane monooxygenase from *Methylococcus capsulatus* (Bath). J Biol Chem 269:14995–15005. https://doi.org/10.1016/S0021-9258(17)36565-1.
9. Nguyen H-HT, Elliott SJ, Yip JH-K, Chan SI. 1998. The particulate methane monooxygenase from *Methylococcus capsulatus* (Bath) is a novel copper-containing three-subunit enzyme: isolation and characterization. J Biol Chem 273:7957–7966. https://doi.org/10.1074/jbc.273.14.7957.
10. Banerjee R, Jones JC, Lipscomb JD. 2019. Soluble methane monooxygenase. Annu Rev Biochem 88:409–431. https://doi.org/10.1146/annurev-biochem-013118-111529.
11. Choi D-W, Kunz RC, Boyd ES, Semrau JD, Antholine WE, Han J-I, Zahn JA, Boyd JM, Arlene M, DiSpirito AA. 2003. The membrane-associated methane monooxygenase (pMMO) and pMMO-NADH: quinone oxidoreductase complex from *Methylococcus capsulatus* Bath. J Bacteriol 185:5755–5764. https://doi.org/10.1128/JB.185.19.5755-5764.2003.
12. Burrows KJ, Cornish A, Scott D, Higgins IJ. 1984. Substrate specificities of the soluble and particulate methane mono-oxygenases of *Methylosinus trichosporium* OB3b. Microbiology 130:3327–3333. https://doi.org/10.1099/00221287-130-12-3327.
13. Stanley S, Prior S, Leak D, Dalton H. 1983. Copper stress underlies the fundamental change in intracellular location of methane mono-oxygenase in methane-oxidizing organisms: studies in batch and continuous cultures. Biotechnol Lett 5:487–492. https://doi.org/10.1007/BF00132233.
14. Prior SD, Dalton H. 1985. The effect of copper ions on membrane content and methane monooxygenase activity in methanol-grown cells of *Methylococcus capsulatus* (Bath). Microbiology 131:155–163. https://doi.org/10.1099/00221287-131-1-155.
15. Gu W, Semrau JD. 2017. Copper and cerium-regulated gene expression in *Methylosinus trichosporium* OB3b. Appl Microbiol Biotechnol 101:8499–8516. https://doi.org/10.1007/s00253-017-8572-2.
16. Choi DW, Zea CJ, Do YS, Semrau JD, Antholine WE, Hargrove MS, Pohl NL, Boyd ES, Geesey GG, Hartsel SC, Shafe PH, McEllistrem MT, Kisting CJ, Campbell D, Rao V, de la Mora AM, Dispirito AA. 2006. Spectral, kinetic, and thermodynamic properties of Cu(I) and Cu(II) binding by methanobactin from *Methylosinus trichosporium* OB3b. Biochemistry 45:1442–1453. https://doi.org/10.1021/bi051815t.
17. DiSpirito AA, Semrau JD, Murrell JC, Gallagher WH, Dennison C, Vuilleumier S. 2016. Methanobactin and the link between copper and bacterial methane oxidation. Microbiol Mol Biol Rev 80:387–409. https://doi.org/10.1128/MMBR.00058-15.
18. Kim HJ, Graham DW, DiSpirito AA, Alterman MA, Galeva N, Larive CK, Asunskis D, Sherwood PM. 2004. Methanobactin, a copper-acquisition compound from methane-oxidizing bacteria. Science 305:1612–1615. https://doi.org/10.1126/science.1098322.
19. Semrau JD, Jagadevan S, DiSpirito AA, Khalifa A, Scanlan J, Bergman BH, Freemeier BC, Baral BS, Bandow NL, Vorobev A, Haft DH, Vuilleumier S, Murrell JC. 2013. Methanobactin and MmoD work in concert to act as the "copper-switch" in methanotrophs. Environ Microbiol 15:3077–3086. https://doi.org/10.1111/1462-2920.12150.
20. Choi DW, Do YS, Zea CJ, McEllistrem MT, Lee S-W, Semrau JD, Pohl NL, Kisting CJ, Scardino LL, Hartsel SC, Boyd ES, Geesey GG, Riedel TP, Shafe PH, Kranski KA, Tritsch JR, Antholine WE, DiSpirito AA. 2006. Spectral and thermodynamic properties of Ag(I), Au(III), Cd(II), Co(II), Fe(III), Hg(II), Mn(II), Ni(II), Pb(II), U(IV), and Zn(II) binding by methanobactin from *Methylosinus trichosporium* OB3b. J Inorg Biochem 100:2150–2161. https://doi.org/10.1016/j.jinorgbio.2006.08.017.
21. El Ghazouani A, Baslé A, Gray J, Graham DW, Firbank SJ, Dennison C. 2012. Variations in methanobactin structure influences copper utilization by methane-oxidizing bacteria. Proc Natl Acad Sci U S A 109:8400–8404. https://doi.org/10.1073/pnas.1112921109.
22. Chi Fru E, Gray N, McCann C, Baptista J, Christgen B, Talbot H, Ghazouani AE, Dennison C, Graham D. 2011. Effects of copper mineralogy and methanobactin on cell growth and sMMO activity in *Methylosinus trichosporium* OB3b. Biogeosciences 8:2887–2894. https://doi.org/10.5194/bg-8-2887-2011.
23. Pesch ML, Hoffmann M, Christl I, Kraemer SM, Kretzschmar R. 2013. Competitive ligand exchange between Cu-humic acid complexes and methanobactin. Geobiology 11:44–54. https://doi.org/10.1111/gbi.12010.
24. Kulczycki E, Fowle DA, Kenward PA, Leslie K, Graham DWRJA. 2007. Methanobactin-promoted dissolution of Cu-substituted borosilicate glass. Geobiology 5:251–263. https://doi.org/10.1111/j.1472-4669.2007.00102.x.
25. Park YJ, Roberts GM, Montaser R, Kenney GE, Thomas PM, Kelleher NL, Rosenzweig AC. 2021. Characterization of a copper-chelating natural product from the methanotroph *Methylosinus* sp. LW3. Biochemistry 60:2845–2850. https://doi.org/10.1021/acs.biochem.1c00443.
26. Whittenbury R, Phillips K, Wilkinson J. 1970. Enrichment, isolation and some properties of methane-utilizing bacteria. Microbiology 61:205–218.
27. Stein LY, Yoon S, Semrau JD, Dispirito AA, Crombie A, Murrell JC, Vuilleumier S, Kalyuzhnaya MG, Op den Camp HJM, Bringel F, Bruce D, Cheng J-F, Copeland A, Goodwin L, Han S, Hauser L, Jetten MSM, Lajus A, Land ML, Lapidus A, Lucas S, Médigue C, Pitluck S, Woyke T, Zeytun A, Klotz MG. 2010. Genome sequence

of the obligate methanotroph *Methylosinus trichosporium* strain OB3b. J Bacteriol 192:6497–6498. https://doi.org/10.1128/JB.01144-10.
28. Semrau JD, DiSpirito AA, Obulisamy PK, Kang-Yun CS. 2020. Methanobactin from methanotrophs: genetics, structure, function and potential applications. FEMS Microbiol Lett 367:fnaa045. https://doi.org/10.1093/femsle/fnaa045.
29. Gu W, Baral BS, DiSpirito AA, Semrau JD. 2017. An aminotransferase is responsible for the deamination of the N-terminal leucine and required for formation of oxazolone ring A in methanobactin of *Methylosinus trichosporium* OB3b. Appl Environ Microbiol 83:e02619-16. https://doi.org/10.1128/AEM.02619-16.
30. Kenney GE, Dassama LMK, Pandelia M-E, Gizzi AS, Martinie RJ, Gao P, DeHart CJ, Schachner LF, Skinner OS, Ro SY, Zhu X, Sadek M, Thomas PM, Almo SC, Bollinger JM, Krebs C, Kelleher NL, Rosenzweig AC. 2018. The biosynthesis of methanobactin. Science 359:1411–1416. https://doi.org/10.1126/science.aap9437.
31. El Ghazouani A, Basle A, Firbank SJ, Knapp CW, Gray J, Graham DW, Dennison C. 2011. Copper-binding properties and structures of methanobactins from *Methylosinus trichosporium* OB3b. Inorg Chem 50:1378–1391. https://doi.org/10.1021/ic101965j.
32. Dassama LM, Kenney GE, Ro SY, Zielazinski EL, Rosenzweig AC. 2016. Methanobactin transport machinery. Proc Natl Acad Sci U S A 113:13027–13032. https://doi.org/10.1073/pnas.1603578113.
33. Gu W, Haque MFU, Baral BS, Turpin EA, Bandow NL, Kremmer E, Flatley A, Zischka H, DiSpirito AA, Semrau JD. 2016. A TonB-dependent transporter is responsible for methanobactin uptake by *Methylosinus trichosporium* OB3b. Appl Environ Microbiol 82:1917–1923. https://doi.org/10.1128/AEM.03884-15.
34. Peng P, Kang-Yun CS, Chang J, Gu W, DiSpirito AA, Semrau JD. 2022. Two TonB-dependent transporters in *Methylosinus trichosporium* OB3b are responsible for uptake of different forms of methanobactin and are involved in the canonical "copper switch." Appl Environ Microbiol 88:e01793-21. https://doi.org/10.1128/AEM.01793-21.
35. Noinaj N, Guillier M, Barnard TJ, Buchanan SK. 2010. TonB-dependent transporters: regulation, structure, and function. Annu Rev Microbiol 64:43–60. https://doi.org/10.1146/annurev.micro.112408.134247.
36. Ferguson AD, Amezcua CA, Halabi NM, Chelliah Y, Rosen MK, Ranganathan R, Deisenhofer J. 2007. Signal transduction pathway of TonB-dependent transporters. Proc Natl Acad Sci U S A 104:513–518. https://doi.org/10.1073/pnas.0609887104.
37. Ferguson AD, Chakraborty R, Smith BS, Esser L, Van Der Helm D, Deisenhofer J. 2002. Structural basis of gating by the outer membrane transporter FecA. Science 295:1715–1719. https://doi.org/10.1126/science.1067313.
38. Koebnik R. 2005. TonB-dependent trans-envelope signalling: the exception or the rule? Trends Microbiol 13:343–347. https://doi.org/10.1016/j.tim.2005.06.005.
39. Kim I, Stiefel A, Plantör S, Angerer A, Braun V. 1997. Transcription induction of the ferric citrate transport genes via the N-terminus of the FecA outer membrane protein, the Ton system and the electrochemical potential of the cytoplasmic membrane. Mol Microbiol 23:333–344. https://doi.org/10.1046/j.1365-2958.1997.2401593.x.
40. Moraleda-Muñoz A, Marcos-Torres FJ, Pérez J, Muñoz-Dorado J. 2019. Metal-responsive RNA polymerase extracytoplasmic function (ECF) sigma factors. Mol Microbiol 112:385–398. https://doi.org/10.1111/mmi.14328.
41. Kenney GE, Rosenzweig AC. 2018. Chalkophores. Annu Rev Biochem 87:645–676. https://doi.org/10.1146/annurev-biochem-062917-012300.
42. Beare PA, For RJ, Martin LW, Lamont IL. 2003. Siderophore-mediated cell signalling in *Pseudomonas aeruginosa*: divergent pathways regulate virulence factor production and siderophore receptor synthesis. Mol Microbiol 47:195–207. https://doi.org/10.1046/j.1365-2958.2003.03288.x.
43. Härle C, Kim I, Angerer A, Braun V. 1995. Signal transfer through three compartments: transcription initiation of the *Escherichia coli* ferric citrate transport system from the cell surface. EMBO J 14:1430–1438. https://doi.org/10.1002/j.1460-2075.1995.tb07129.x.
44. Schalk IJ, Yue WW, Buchanan SK. 2004. Recognition of iron-free siderophores by TonB-dependent iron transporters. Mol Microbiol 54:14–22. https://doi.org/10.1111/j.1365-2958.2004.04241.x.
45. Schulz S, Eckweiler D, Bielecka A, Nicolai T, Franke R, Dötsch A, Hornischer K, Bruchmann S, Düvel J, Häussler S. 2015. Elucidation of sigma factor-associated networks in *Pseudomonas aeruginosa* reveals a modular architecture with limited and function-specific crosstalk. PLoS Pathog 11:e1004744. https://doi.org/10.1371/journal.ppat.1004744.
46. Rushworth DD, Christl I, Kumar N, Hoffmann K, Kretzschmar R, Lehmann MF, Schenkeveld WD, Kraemer SM. 2022. Copper mobilisation from Cu sulphide minerals by methanobactin: effect of pH, oxygen and natural organic matter. Geobiology 20:690–706. https://doi.org/10.1111/gbi.12505.
47. Bandow NL, Gallagher WH, Behling L, Choi DW, Semrau JD, Hartsel SC, Gilles VS, DiSpirito AA. 2011. Isolation of methanobactin from the spent media of methane-oxidizing bacteria. Methods Enzymol 495:259–269. https://doi.org/10.1016/B978-0-12-386905-0.00017-6.
48. Krentz BD, Mulheron HJ, Semrau JD, Dispirito AA, Bandow NL, Haft DH, Vuilleumier S, Murrell JC, McEllistrem MT, Hartsel SC, Gallagher WH. 2010. A comparison of methanobactins from *Methylosinus trichosporium* OB3b and *Methylocystis* strain SB2 predicts methanobactins are synthesized from diverse peptide precursors modified to create a common core for binding and reducing copper ions. Biochemistry 49:10117–10130. https://doi.org/10.1021/bi1014375.
49. Vorobev A, Jagadevan S, Baral BS, DiSpirito AA, Freemeier BC, Bergman BH, Bandow NL, Semrau JD. 2013. Detoxification of mercury by methanobactin from *Methylosinus trichosporium* OB3b. Appl Environ Microbiol 79:5918–5926. https://doi.org/10.1128/AEM.01673-13.
50. Welander PV, Summons RE. 2012. Discovery, taxonomic distribution, and phenotypic characterization of a gene required for 3-methylhopanoid production. Proc Natl Acad Sci U S A 109:12905–12910. https://doi.org/10.1073/pnas.1208255109.
51. Schäfer A, Tauch A, Jäger W, Kalinowski J, Thierbach G, Pühler A. 1994. Small mobilizable multi-purpose cloning vectors derived from the *Escherichia coli* plasmids pK18 and pK19: selection of defined deletions in the chromosome of *Corynebacterium glutamicum*. Gene 145:69–73. https://doi.org/10.1016/0378-1119(94)90324-7.
52. Simon R. 1984. High frequency mobilization of gram-negative bacterial replicons by the *in vitro* constructed Tn 5-Mob transposon. Mol Gen Genet 196:413–420. https://doi.org/10.1007/BF00436188.
53. Martin H, Murrell J. 1995. Methane monooxygenase mutants of *Methylosinus trichosporium* constructed by marker-exchange mutagenesis. FEMS Microbiol Lett 127:243–248. https://doi.org/10.1111/j.1574-6968.1995.tb07480.x.
54. Bandow N, Gilles VS, Freesmeier B, Semrau JD, Krentz B, Gallagher W, McEllistrem MT, Hartsel SC, Choi DW, Hargrove MS, Heard TM, Chesner LN, Braunreiter KM, Cao BV, Gavitt MM, Hoopes JZ, Johnson JM, Polster EM, Schoenick BD, Umlauf AM, DiSpirito AA. 2012. Spectral and copper binding properties of methanobactin from the facultative methanotroph *Methylocystis* strain SB2. J Inorg Biochem 110:72–82. https://doi.org/10.1016/j.jinorgbio.2012.02.002.
55. Peng P, Zheng Y, Koehorst JJ, Schaap PJ, Stams AJ, Smidt H, Atashgahi S. 2017. Concurrent haloalkanoate degradation and chlorate reduction by *Pseudomonas chloritidismutans* AW-1^T. Appl Environ Microbiol 83:e00325-17. https://doi.org/10.1128/AEM.00325-17.
56. Schmittgen TD, Livak KJ. 2008. Analyzing real-time PCR data by the comparative C_T method. Nat Protoc 3:1101–1108. https://doi.org/10.1038/nprot.2008.73.
57. Kalidass B, Ul-Haque MF, Baral BS, DiSpirito AA, Semrau JD. 2015. Competition between metals for binding to methanobactin enables expression of soluble methane monooxygenase in the presence of copper. Appl Environ Microbiol 81:1024–1031. https://doi.org/10.1128/AEM.03151-14.
58. Sullivan MJ, Petty NK, Beatson SA. 2011. Easyfig: a genome comparison visualizer. Bioinformatics 27:1009–1010. https://doi.org/10.1093/bioinformatics/btr039.
59. El-Gebali S, Mistry J, Bateman A, Eddy SR, Luciani A, Potter SC, Qureshi M, Richardson LJ, Salazar GA, Smart A, Sonnhammer ELL, Hirsh L, Paladin L, Piovesan D, Tosatto SCE, Finn RD. 2019. The Pfam protein families database in 2019. Nucleic Acids Res 47:D427–D432. https://doi.org/10.1093/nar/gky995.
60. Im J, Lee SW, Yoon S, DiSpirito AA, Semrau JD. 2011. Characterization of a novel facultative *Methylocystis* species capable of growth on methane, acetate and ethanol. Environ Microbiol Rep 3:174–181. https://doi.org/10.1111/j.1758-2229.2010.00204.x.